Dissociative Ionization of Methyl Chloride and Methyl Bromide by Collision with Metastable Neon Atoms

B. Brunetti,* P. Candori, J. De Andres,† and F. Pirani

Dipartimento di Chimica, Universita' di Perugia, 06100 Perugia, Italy

M. Rosi, S. Falcinelli, and F. Vecchiocattivi*

Istituto per le Tecnologie Chimiche, Universita' di Perugia, 06100 Perugia, Italy

Received: March 14, 1997; In Final Form: May 20, 1997[⊗]

Total and partial cross sections for Penning ionization of methyl chloride and methyl bromide by metastable neon atoms have been measured as a function of collision energy in the 0.040−0.15 eV range. The partial cross sections for the formation of CH_3X^+, CH_3^+, and CH_2X^+ (X = Cl, Br) show a decreasing trend, with different slopes, when the collision energy increases. The branching ratios indicate that the production of fragment ions is favored at higher energies. Based on new correlation rules that allow to estimate pure van der Waals but also charge-transfer contributions to intermolecular potentials, the anisotropy of the Ne*−CH_3Cl interaction has been semiempirically estimated. Within the electron exchange model of Penning ionization, it is shown that the anisotropy of interaction, together with the anisotropy of electron distribution of the orbitals involved in ionization, is correlated with the behavior of the ionization cross sections and branching ratios as a function of collision energy. In particular, the presence of the attractive interaction at the two ends of the molecule is responsible for the decreasing energy dependence of the total ionization cross sections, while a softer repulsive wall around the methyl group is responsible for the increase of fragment ions when collision energy increases.

I. Introduction

The collision of an excited atom, A*, with a target molecule, BC, characterized by an ionization potential lower than the atom excitation energy, leads to autoionization of the intermediate [A*···BC] complex. The product of autoionization, the ionic complex [A···BC^+], then continues the collision, leading to the formation of different ions. Behind the formation of BC^+ ions in different vibronic states (Penning ionization) and associate ions ABC^+ (associative ionization), an ion−molecule reaction between ground state A and BC^+ can occur (rearrangement ionization), as well as dissociation of excited BC^+ molecular ions (dissociative ionization).

These collisional autoionization processes, generally known as Penning ionization, have been the subject of several experimental and theoretical studies during the past years, and recently, two review articles have summarized the most important conclusions that have been drawn.[1,2]

Experimental studies on the dynamics of autoionization of collisional complexes can be worked out by measuring different observables such as the kinetic energy spectra of the electrons emitted, the collision energy dependence of total and partial (Penning, associative, rearrangement, and dissociative) ionization cross sections, or even the electron energy spectra in coincidence with the specific ion produced.

From the theoretical point of view, these processes can be simply discussed on the basis of the so-called optical model, where the interaction between the neutral collision partners is described by a local complex potential, depending only on the internuclear coordinates, whose real part represents the interaction potential of the particles and the imaginary part represents the probability of autoionization of the system. This model has been successfully applied for rigorous quantum mechanical treatments of Penning ionization of atoms.[1−4] The corresponding application to molecules requires also the knowledge of the angular dependence of both the real and imaginary part of the optical potential. Recent attempts have been made for a rigorous treatment of He*(2^1S,2^3S)−H_2 by the use of a complex potential energy surface for the interaction in the entrance channel and an another potential energy surface for the interaction of the collision partners in the second step.[5] Very recently, quantum mechanical models[6,7] and quasiclassical trajectory methods have been also attempted.[8]

Anisotropy effects are expected to be very significant in Penning ionization of molecules. This can be easily understood when the commonly accepted electron exchange mechanism, originally proposed by Hotop and Niehaus,[9] is taken into account. This mechanism implies that ionization occurs, mainly at the turning point, through a transfer of an outer-shell electron of the molecule into the inner-shell vacancy of the excited rare gas, which in turn ejects the external electron. On the basis of this process, where the overlapping of the proper orbitals of the metastable and the target is a crucial condition, it is quite evident that the orientation of the molecule with respect to the incoming metastable atom can be of great importance in determining the ionization probability, together with the symmetry of the outer-shell electron orbitals of the target. In fact, a metastable atom approach along a given direction can lead to a preferential removal of the electron from a specific orbital characterized by an electron density distribution extended toward the incoming metastable atom.

This aspect stimulated some recent experimental studies devoted to clarify the role of the anisotropy of interaction and the possible stereospecificity of the collisional autoionization dynamics. Ohno and co-workers[10−13] recently measured the state-resolved collision energy dependences of Penning ionization cross sections for collisions of He*(^3S) with some simple

† On leave from Departament de Quimica Fisica, Universitat de Barcelona, Spain.

⊗ Abstract published in *Advance ACS Abstracts,* September 15, 1997.

S1089-5639(97)00945-6 CCC: $14.00 © 1997 American Chemical Society

molecules, detecting energy-analyzed electrons as functions of metastable helium velocity. They found that the ionization cross sections for the population of specific electronic states of the primary ion can show strongly different energy dependences, according to the distribution of electron densities of the involved orbitals and the anisotropy of interaction between the metastable atom and the molecular target. Similar effects were found by Siska and co-workers, who measured[14] and analyzed[15] the vibronic populations of N_2^+ in a Penning ionization electron spectroscopy experiment on the $He^*(^1S)-N_2$ system. Also in this case, the vibrationally resolved collisional energy dependence of the spectra was correlated with the role of the anisotropy of interaction combined with the spatial distribution of the molecular orbitals.

In this paper, a study on the dissociative ionization of CH_3Cl and CH_3Br molecules by collision with $Ne^*(^3P_{2,0})$, in the range between 0.04 and 0.15 eV is reported. The ionization of these molecules gives rise to a fragmentation that appears correlated, from photoionization studies available in the literature, with the possible electronic states of the molecular ions produced. Therefore, it is possible to attribute each product ion to the formation of CH_3Cl^+ and CH_3Br^+ primary ions in a specific electronic state.

The velocity dependence of cross sections and branching ratios for Penning and dissociative ionization in $Ne^*(^3P_{2,0})-CH_3Cl$, CH_3Br collisions have been measured. For comparison, the corresponding processes with methane have been also studied. The experimental results are discussed considering different combinations of the anisotropy of interaction between the neutral reactants and the spatial electron density distributions of the molecular orbitals involved in the ionization dynamics. For this purpose, electron density distribution maps have been obtained, for the CH_3Cl molecule, by using standard quantum chemistry codes, while the anisotropy of interaction has been estimated from correlation rules recently developed in our laboratory.

II. Experimental Section

The apparatus used for the present measurements has been described previously in detail.[16,17] Basically, it consists of a supersonic or effusive metastable neon atom beam that crosses at right angles an effusive secondary beam produced by a microcapillary array. The metastable atom beam is detected by a channel electron multiplier located along the beam path, while the target beam is monitored by a total ionization detector. The ions produced in the collision zone are extracted, focused, mass analyzed by a quadrupole filter, and then detected by an other channel electron multiplier.

The neon beam can be produced by two sources that can be used alternately. The first one is a standard effusive source at room temperature while the second is a supersonic source that can be heated to different temperatures. The metastable atoms are produced by electron bombardment at ≈150 eV; the bombardment is expected to yield $Ne^*(^3P_2)$ and $Ne(^3P_0)$ in a population close to the statistical ratio 5:1.

The metastable atom velocity can be analyzed by a time-of-flight (TOF) technique: the beam is pulsed by a rotating slotted disk, and the metastable atoms are counted, using a multiscaler, as a function of the delay time from the beam opening.

The velocity dependence of the cross sections can be obtained by two different methods. In the first method the effusive neon beam is used together with the TOF setup: Time delay spectra of the metastable atom arrival at the collision zone are recorded, as well as the time spectra of the intensity of product ions, and then the relative cross sections as a function of collision energy, $\sigma(E)$, are obtained for a given delay time, τ, according to the equation

$$\sigma(E) = N^+(\tau)v^*/N^*(\tau)v_r$$

where N^+ and N^* are the intensities of the product ions and metastable atom, respectively, and v^* and v_r are the corresponding metastable atom and relative velocities.

By the second method a supersonic beam of metastable neon atoms is directly crossed with the target beam. The supersonic beam is well-defined in velocity ($\Delta v/v \approx 0.1$) and therefore the cross sections are again obtained by the above equation, where N^+ and N^* are now simply the total intensity of the product ions and the full beam metastable intensity, respectively. By this method, the collision energy dependence of the cross sections is obtained by varying the nozzle temperature of the supersonic source.

The two methods are equivalent and were both used to carry out the present measurements. The first method allowed us to obtain the $\sigma(E)$ dependence in a single experiment, while the second, which requires an experiment for each single collision energy E, allowed us to work with higher intensity signals.

The collision energy dependence of the branching ratios is measured by changing the nozzle temperature of the supersonic neon beam and recording the relevant mass spectra of the product ions. In these experiments, mass spectra are corrected for the nonnegligible contribution to ionization due to photons produced in the metastable excitation zone.

The photoionization branching ratios are recorded by replacing the neon beam source with a microwave discharge in pure neon. Such discharge produces exclusively Ne I photons (16.96 and 16.76 eV), the metastable atoms being quenched by collision on the wall of a long capillary tube located after the discharge.

The measurement of relative abundancies of product ions in quadrupole mass spectrometry is known to be subject to possible errors due to different ion transmission through the mass filter and ion collection efficiencies. Errors on ion collection efficiency have been minimized by the use of proper ion extraction and acceleration fields. The ion transmission of the mass filter for the dissociative ionization of methyl halides have been calibrated by taking as a reference the fragmentation patterns in He I photoionization of CH_3Cl and CH_3Br as measured by Eland *et al.*[18] He I dissociative photoionization has been measured simply by sending pure helium in the microwave discharge mentioned above. No calibration is necessary for methane since the spectrum is characterized by three adjacent masses. For this reason, the error in the determination of methane ionization branching ratio is definitely lower, in the present experiment, than in the case of methyl halides (see Table 1).

III. Results and Discussion

In Table 1, the ionization fragmentation patterns by Ne I photons and $Ne^*(^3P_{2,0})$ atoms, at an average collision energy of around 0.045 eV, are reported for CH_4, CH_3Cl, and CH_3Br, as measured in the present experiment. To check the best experimental conditions, the fragmentation patterns of C_2H_6 have been also measured. The results obtained in other laboratories[19−24] are reported for comparison. No comparison is made for CH_3Cl and CH_3Br because, to our knowledge, no data of this type are available in the literature.

It appears that $Ne^*(^3P_{2,0})-CH_4$ collisional autoionization leads to CH_4^+, CH_3^+, and CH_2^+ ions, with a fragmentation pattern very similar to that of Ne I photoionization, but characterized by a small evident higher fragmentation. (A higher fragmenta-

TABLE 1: Ion Fragmentation Patterns by Ne I Photons and Neon Metastable Atoms

		Ne I					Ne*($^3P_{2,0}$)		
		this work	*a*	*b*	*c*	*d*	this work	*e*	*f*
CH_4	CH_4^+	51.1 (±4%)	51.2	49.5	46.8		48.1 (±4%)	43.3	52.4
	CH_3^+	46.2 (±4%)	47.1	48.0	51.0		50.0 (±4%)	52.4	45.0
	CH_2^+	2.7 (±4%)	1.7	2.5	2.2		1.9 (±4%)	4.3	2.6
C_2H_6	$C_2H_6^+$	14.3 (±4%)			11.3	14.5	8.7 (±4%)	7.3	8.0
	$C_2H_5^+$	13.0 (±4%)			12.6	13.1	14.2 (±4%)	12.7	14.5
	$C_2H_4^+$	55.0 (±4%)			59.5	55.2	48.4 (±4%)	49.2	44.0
	$C_2H_3^+$	11.5 (±4%)			10.9	10.6	18.1 (±4%)	18.7	15.1
	$C_2H_2^+$	5.0 (±4%)			4.7	5.0	8.2 (±4%)	9.5	13.6
	CH_3^+	1.2 (±4%)			1.0	1.6	2.4 (±4%)	2.6	4.8
CH_3Cl	CH_3Cl^+	58 (±15%)					59 (±15%)		
	CH_2Cl^+	8 (±15%)					8 (±15%)		
	CH_3^+	34 (±15%)					33 (±15%)		
CH_3Br	CH_3Br^+	53 (±25%)					57 (±25%)		
	CH_2Br^+	19 (±25%)					18 (±25%)		
	Br^+	1 (±25%)					1 (±25%)		
	CH_3^+	27 (±25%)					24 (±25%)		

[a] Reference 19. [b] Reference 20. [c] Reference 21. [d] Reference 22. [e] Reference 23. [f] Reference 24.

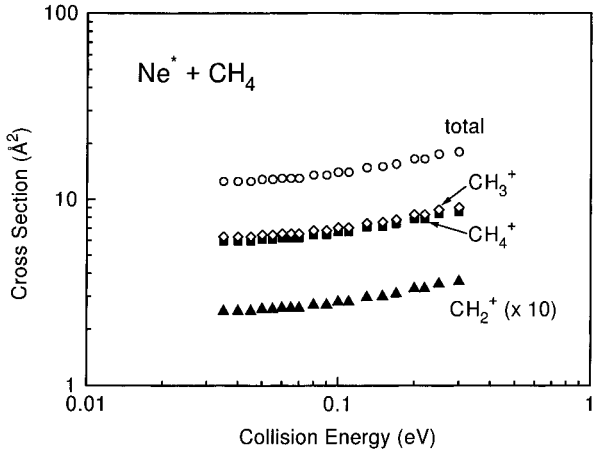

Figure 1. Total and partial ionization cross sections for collision of metastable neon atom with methane molecules as a function of the relative collision energy.

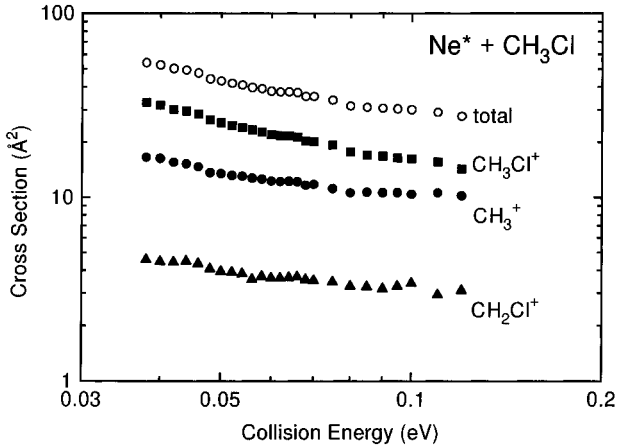

Figure 2. Total and partial ionization cross sections for collision of metastable neon atom with methyl chloride molecules as a function of the relative collision energy.

tion has been also found in the case of C_2H_6.) In Ne*($^3P_{2,0}$)−CH_3Cl ionization, CH_3Cl^+, CH_3^+, and CH_2Cl^+ ions are mainly formed while, in Ne*($^3P_{2,0}$)−CH_3Br collisions, CH_3Br^+, CH_3^+, CH_2Br^+, and Br^+ ions are produced. For these molecules, other fragments may be present in the spectrum, but contributions of ions to an extent lower than 1% have been neglected here because it is not possible to study their collision energy dependence. For both the methyl halides the fragmentation pattern is similar to that obtained in the corresponding photoionization.

In Figures 1, 2, and 3, total and partial ionization cross sections, for the three systems studied, are reported as a function of collision energy. Total ionization cross sections for these molecules[17,25] have been already measured in our laboratory, and the present results are in full agreement with the previous ones. Partial ionization cross sections are reported for the first time. Total and partial ionization cross sections of the methyl halides show a decreasing energy dependence. On the contrary, those of methane increase as collision energy increases.

In Figures 4, 5, and 6 branching ratios for the formation of the various ions are shown as a function of collision energy. It can be noted again that a different behavior of methyl halides is present when compared with that of methane. While the fraction of fragment ions CH_3^+ and CH_2X^+ increases with collision energy for methyl halides, no variation of branching ratios is observed for methane in the whole energy range investigated.

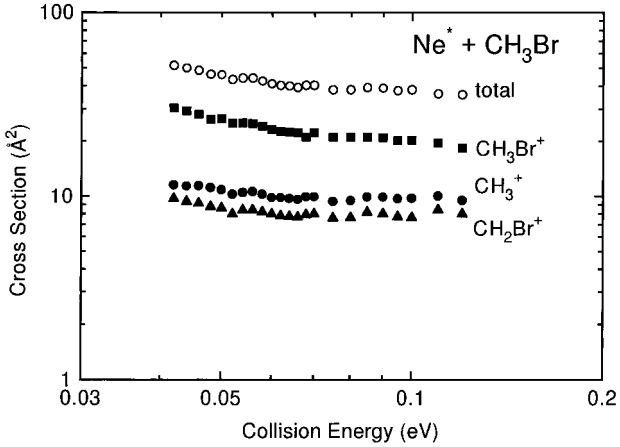

Figure 3. Total and partial ionization cross sections for collision of metastable neon atoms with methyl bromide molecules as a function of the relative collision energy.

As will be shown below, ionization cross sections and branching ratios can be interpreted in terms of the collision dynamics of the neon metastable atoms with the target molecules. In particular, for the methyl halides, the behavior of the branching ratio as a function of collision energy can be attributed to the anisotropy of the interaction associated with the anisotropy of the electron density distribution of the orbitals involved in ionization.

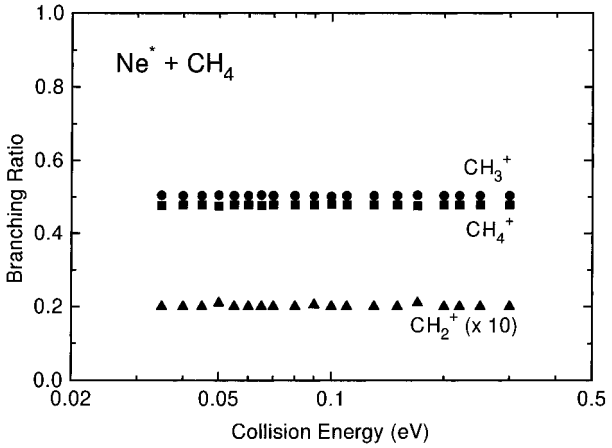

Figure 4. Branching ratio for each product ion produced in the ionization of methane molecules by collision with metastable neon atoms as a function of the relative collision energy.

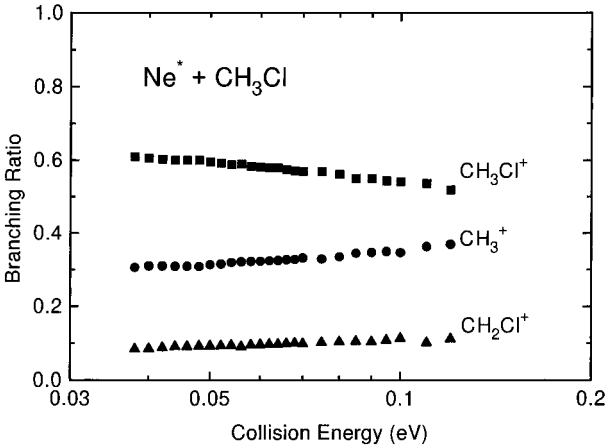

Figure 5. Branching ratio for each product ion produced in the ionization of methyl chloride molecules by collision with metastable neon atoms as a function of the relative collision energy.

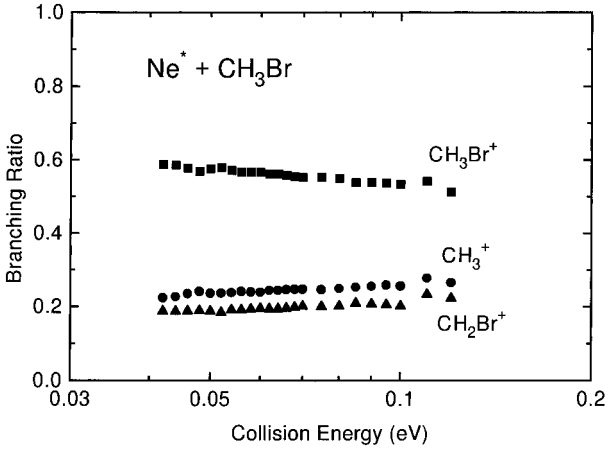

Figure 6. Branching ratio for each product ion produced in the ionization of methyl bromide molecules by collision with metastable neon atoms as a function of the relative collision energy.

A. Methane Ion Fragmentation. The electronic structure of methane may be written as $(1s\ a_1)^2(2s\ a_1)^2(2p\ t_2)^6$. The two lowest ionization potentials of the molecule are 12.7 and 22 eV, corresponding to the ejection of one electron from the 2p t_2 and 2s a_1 orbitals, respectively.[26] Therefore, at energies between 12.7 and 22 eV, only ground state nascent CH_4^+ ions can be formed. Since the energy available in this experiment is about 16.7 eV, the observed fragmentation to CH_3^+ and CH_2^+ must arise from this ground state nascent ion. In fact, theoretical considerations[27] indicate that, when an electron is removed from the 2p t_2 orbital, the CH_4^+ ion, initially in a triply degenerate state of T_d symmetry, undergoes a Jahn−Teller distortion to more stable states, characterized by different symmetries. In particular, the distortions to C_{3v} and C_{2v} symmetries represent the possible path toward CH_3^+ and CH_2^+, respectively. Fragmentation processes of CH_4^+ have been studied by Stockbauer[28] and by Bombach *et al.*[29] by using a photoelectron−photoion coincidence technique. By these studies, breakdown diagrams have been obtained, where the fragmentation pattern of the ground state ion primarily produced is related to its internal energy. These diagrams show that only CH_4^+ is produced when the nascent ion is formed with an internal energy lower than 1.6 eV. Then, when the internal energy increases, CH_3^+ and CH_2^+ ions appear, with thresholds of 1.6 and 2.5 eV.

As in photoionization, a Jahn−Teller distortion must be responsible of the observed fragmentation in Ne*($^3P_{2,0}$)−CH_4. However, the fragmentation is slightly higher than in photoionization, and it is likely that this difference is due to the interaction between the two collision partners. Two explanations are possible: (I) the van der Waals interaction between the metastable neon atoms and methane leads to nascent CH_4^+ ions characterized by a slightly higher internal energy; (II) the strong ion-induced dipole interaction between ground state neon atoms and CH_4^+, after the electron ejection, facilitates the Jahn−Teller distortion. To analogous conclusions came Sieck and Gorden,[21] who compared their measurements of the fragmentation patterns in He I and Ne I photoionization of simple hydrocarbons with the corresponding results in Penning ionization, measured in other laboratories. The present comparison for Penning and photoionization of methane, performed within the same experiment and therefore at identical experimental conditions, supports their previous observations.

B. Methyl Halide Ion Fragmentation. Substantially different is the situation of the two halogenated substitutes, CH_3Cl and CH_3Br. Their electronic structure can be derived from that of methane. The substitution of an hydrogen with an halogen reduces the symmetry of the system from T_d to C_{3v} and splits the pt_2 orbital to $(\pi_e)^4(\sigma a_1)^2$. The inclusion of the outer orbitals of the halogen gives the following sequence: $(\text{core})...(\pi_e)^4(\sigma a_1)^2(np\pi_{eX})^4$, where X = Cl, Br and n = 3, 4.[26] At the energy available in the present experiment CH_3Cl^+ and CH_3Br^+ ions can be produced in the ground state (X) and in the first two excited states (A and B). These ions are formed when an electron is ejected from each one of the three last occupied external orbitals. The formation of the ground state ion correspond to the removal of one electron from the highest occupied orbital, $(np\pi_{eX})$, largely localized on the halogen atom (giving an ion in a ^2E state subject to spin−orbit coupling and Jahn−Teller effects). The first excited $CH_3X^+(A)$ ion is produced by the removal of one electron from the (σa_1), which is a carbon−halogen bonding orbital. Finally, the $CH_3X^+(B)$ state is populated when an electron is lost by the (π_e) orbital, largely localized on the methyl group. In order to have a clear view of the localization of the various orbitals, the electron densities of the three last occupied orbitals of CH_3Cl are shown in Figure 7. The basis set employed in the *ab initio* calculations is of triple-zeta valence quality,[31,32] augmented with a polarization function. A d-type polarization function was used for the chlorine atom (exponent 0.619)[33] and the carbon atom (exponent 0.72),[33] while a p-type polarization function (exponent 1.00)[33] was used for the hydrogen atoms. The geometry of the molecule has been optimized at the SCF level, assuming a C_{3v} symmetry, using gradient techniques. The calculations were performed by

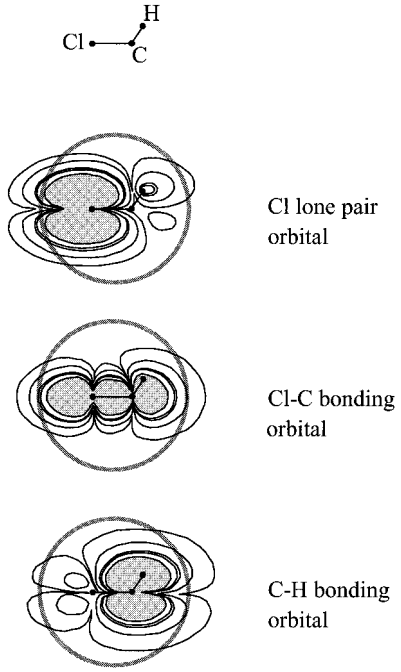

Figure 7. Contour maps of the electron spatial distribution of the three outer molecular orbitals in CH_3Cl involved in the ionization by collision with metastable neon atoms. The van der Waals average size of the molecule is also shown in order to indicate the parts of the orbitals that can be more efficiently "ionized" by metastable neon atoms.

the use of the GAMESS[34] program package implemented on a cluster of IBM RS6000 workstations.

The energy of the orbitals, symmetries, ionization potentials, adiabatic correlation diagrams, Jahn−Teller distortions, and vibrational motions of these ions have been established by several previous works.[26] Among these, particularly interesting are the works of Eland *et al.*[18] and Lane and Powis,[34] who performed photoelectron−photoion coincidence studies on the dynamics of methyl halide ion dissociations. They showed that when these ions are formed in different electronic states, they undergo specific reactions to different products. According to these measurements, CH_3Cl^+ and CH_3Br^+ formed in the ground state remain substantially undissociated, while the same ions excited to the A and B states fully dissociate to fragments. In particular, CH_3Cl^+(A) leads completely to CH_3^+, with a large kinetic energy release of around 0.4 eV, while CH_3Cl^+(B) gives rise partially to CH_3^+, through an internal conversion from B to A, and partially to CH_2Cl^+ by specific dissociation from B. It has been estimated that 80% of CH_3Cl^+(B) leads to internal conversion to the A state and 20% to specific dissociation toward CH_2Cl^+.

Eland *et al.*[18] did not measure the full breakdown diagram for CH_3Br^+ because of the deleterious effect of this compound on the coincidence apparatus. However, Lane and Powis[34] in their coincidence measurements at individual electron energies showed that the X state remains substantially undissociated while both A and B states undergo essentially statistical fragmentation to CH_3^+ and CH_2Br^+. Br^+ was a minor product and was not taken into account.

In light of these results, the analogies in the fragmentation patterns, reported in Table I, suggest that the X, A, and B states of the ions are populated in a similar ratio both in Ne I photoionization and in Ne*($^3P_{2,0}$) Penning ionization. As a matter of fact, similar electron energy spectra have been experimentally observed also for the case of helium metastables and He I photoionization of methyl halides.[35]

C. The Ne*−CH_3Cl Interaction Potential. Once we discuss the dynamics leading to the observed fragmentation patterns, before discussing the ionization cross sections and their energy dependence, it is helpful to consider the interaction potential between neon metastable atoms and methyl halides. To this effort, the case of Ne*−CH_3Cl has been chosen as a prototype, and then the interaction potential curves for the metastable neon atom approaching the methyl chloride molecule along five different directions have been estimated by using the semiempirical correlation rules, recently developed by Pirani and co-workers.[36−42] The basic principles of these rules are outlined in the following.

The potential energy surface describing the interaction between a neon metastable atom and a methyl halide molecule can be assumed to be determined by two main contributions: a weak van der Waals (vdW) component and a "charge transfer" (CT) interaction. The vdW component represents the electrostatic contribution given by a critical balancing between the long-range attraction, produced by induction and dispersion forces, and the short-range repulsion, produced by the "size" of the outer electron charge distribution of the two partners. The CT term is associated with a configuration mixing that occurs between the neutral Ne*···CH_3Cl system and the lowest excited ionic state $Ne^+\cdots CH_3Cl^-$, this being strongly attractive at intermediate and long range. By using an "educational chemistry" language, one can say that the CT term represents the stabilization due to the resonance between neutral and ionic forms.

In previous studies on atom−atom systems, the whole vdW interaction has been found to be correlated with the polarizability of both the interacting particles, since this property is mainly related to the repulsion through the size of outer electronic orbitals[43] and to the attraction through the terms of a multipolar series.[37,44] Correlation formulas based on the polarizability have been proposed[36,38] and extensively tested for the description of vdW potential features such as R_m, distance of the potential energy minimum, and ϵ, the well depth at R_m. An important point connected with these studies is that, at the distance σ, defined as the distance where the potential vanishes, since attraction and repulsion are balanced, both these two opposite contributions are correlated to ϵ.[43] Since the repulsion is also assumed to be proportional to the sum of the square of the total overlap integral of the valence orbitals,[45,46] the ϵ parameter can be taken as a measure of this sum at the distance σ.

These correlation formulas have been also used for a representation of the main features of the potential energy surface in atom−homonuclear diatom systems. In this case the polarizability is anisotropic being related to the electronic charge distribution of the molecular bond, which can be represented by an ellipsoid form.[40,41] The extension to atom−polyatomic molecule systems has also been studied. This extension is possible by summing the relative contributions of the interaction of each bond. Such contributions depend on the polarizability (average value and anisotropy) of the bond and its orientation and distance from a reference axis.

Correlation rules of the latter type have been applied to the present case to determine the vdW component of the Ne*−CH_3Cl interaction. Each reference axis is assumed to pass through the middle point of the C−Cl bond, which is also close to the center of mass of the molecule, while the polarizability data relative to C−H and C−Cl bonds are taken from refs 43 and 47.

However, as mentioned above, the extension of these rules to polyatomic molecules like halogenated hydrocarbons implies the addition of a CT effect to the vdW component. This effect

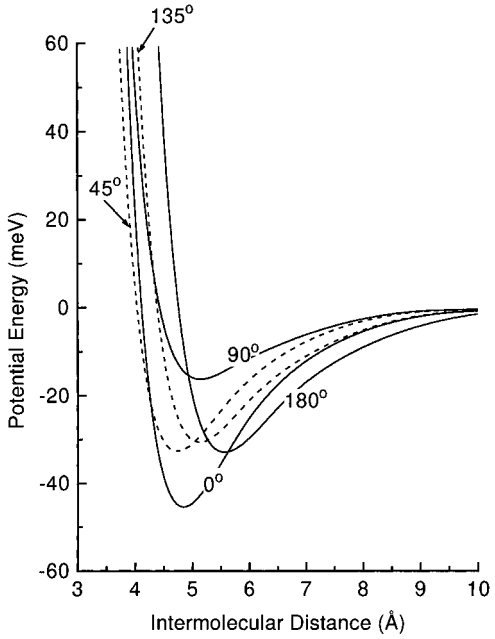

Figure 8. Intermolecular potential energy curves for the interaction between a metastable neon atom and a methyl chloride molecule. The distance is between the nucleus of Ne* and the center of the C−Cl bond in the CH_3Cl molecule. The angles are referred to the direction of the C−Cl bond with the approach to the Cl side as 0°. The potential energy curves have been estimated by averaging over the rotation of the C−H bonds around the C−Cl axis.

can be obtained from the quantum mechanical problem of two interacting states, which is analytically solvable. On this ground, the amount of the configuration interaction is found to depend on the coupling matrix element and on the energy separation between the two states, which is given asymptotically by the difference between the ionization potential of Ne* and the electron affinity of CH_3Cl. Magee[48] has shown that at large distances the coupling matrix element between neutral and ionic states depends on the overlap integral between the two orbitals describing the electron before and after the transfer. Moreover, Grice and Herschbach[49] suggested that, in molecules containing halogen atoms, the overall electronic charge distribution is not substantially modified by the addition of a further electron. It follows that the square of the overlap integral of the transferred electron is practically proportional to the sum of the squares of the overlaps in neutral−neutral systems. On this ground, a correlation formula between the coupling matrix element at σ and ϵ parameters has been developed, tested on other known systems,[42] and applied to the present case.

The intermolecular potential has been computed for 0°, 45°, 90°, 135°, and 180° angles of approach of Ne* to CH_3Cl. In such a calculation the CT effect has been added by taking an exponential dependence on the intermolecular distance and a square cosine angular dependence. This implies that the highest CT effect occurs for the two possible collinear approaches to the C−Cl bond, since the negative molecule is formed when an electron jumps into the lowest C−Cl σ-antibonding orbital. The assumption of a CT angular dependence on the square cosine of the angle of approach takes into account that the σ-antibonding orbital has a cylindrical symmetry.

The obtained potential energy curves, for the various approaches of neon metastable atoms to the center of mass of CH_3Cl, are reported in Figure 8. These curves have been plotted by assuming a Lennard-Jones potential model splined with a long-range $-C_6/R^6$ attraction.

The comparison between the curves at 0°, 90°, and 180° indicates that the presence of the CT contribution introduces a large anisotropy effect in the interaction. In particular: (I) *end-on* approaches, both toward the end of the chlorine atom and the methyl group (0° and 180°), give rise to potential wells much deeper than those corresponding to a *side-on* approach at 90°; (II) the three hydrogen atoms of the methyl group maintain the Ne*($^3P_{2,0}$) atom far from the carbon atom, hampering the effectiveness of the CT and leading to a less deep potential well (around 30%) than in the part of chlorine atom; (III) the repulsive branch at the end of the methyl group is softer than the one at the end of chlorine atom.

Very recently, an *ab initio* calculation about the He*−CH_3-Cl interaction has been reported by Tokue *et al.*[50] Because of the analogies with the present Ne*−CH_3Cl system, a comparison with those results is here commented on. First of all, it has to be noted that in both cases the order of magnitude of the average interaction is similar and falls in the range typical of van der Waals forces with an additional weak "chemical" contribution. However, the potential well around the methyl group found here for Ne*−CH_3Cl is not present in the Tokue *et al.*[50] calculation on He*−CH_3Cl. Moreover, the *ab initio* results on He*−CH_3Cl show a potential minimum at about 90° on the Cl side, and this feature has not been observed in the present estimate on Ne*−CH_3Cl. The differences on the side of the methyl group arise from the fact that the *ab initio* computation has been performed using an MP2 approximation, and in such a scheme, configuration interactions are introduced simply as a perturbation in an Hartree−Fock calculation. However, in the present case the configuration mixing with the ionic $Ne^+-CH_3Cl^-$ state, which is expected to be the main anisotropic contribution in the well region, is considered explicitly. On the other hand, the *ab initio* potential minimum at 90° close to the Cl atom arises from an helium 2s−2p hybridyzation which is known to influence the interaction of helium metastable atoms with several targets.[12,13,15] Similar hybridization effects, which cannot be excluded at very short distances, have been characterized to play a substantially minor role in the case of metastable neon atoms[51] and for this reason have been neglected in the present determination. In any case, the observed discrepancies do not challenge the considerations that will be done in the following.

D. Ionization Cross Sections. Total and partial ionization cross sections show an increase for methane and a decrease for CH_3Cl and CH_3Br with increasing collision energy.

The differences in the energy dependence of total ionization cross sections can be attributed to differences in the interaction potential of the collision partners.[17] It has been well established[52] that in general total ionization cross sections show a decreasing behavior as a function of collision energy when the collision probes the attractive branch of the potential, while showing an increasing trend when the repulsive wall of the potential is probed. A second decreasing trend at higher energies is also expected when the collision probes the hard-core limit of the potential. Starting from these considerations, it has been shown that thermal energy collisions of neon metastable atoms with a weak (and therefore rapidly repulsive) van der Waals interaction with the target lead to increasing cross sections, while collisions characterized by a stronger attractive interaction lead to a decreasing trend.[17]

The increasing or decreasing energy dependence of total ionization cross sections by Ne*($^3P_{2,0}$) has been also correlated to the σ or π symmetry of the molecular orbital of the electron to be removed.[53] Due to their different spatial extent, ionization from σ orbitals should lead to increasing cross sections, while that from π orbitals leads to decreasing cross sections. In terms of the optical model, commonly used to describe collisional

autoionization processes, these indications implicitly assume that the energy dependence of total ionization cross section is strongly influenced by the autoionization width, that is, the imaginary part, of the optical potential.

In order to establish whether the observed differences in the slopes of total ionization cross sections are to be connected more with the nature of the real part of the optical potential than the imaginary part, blank tests have been performed by calculating ionization cross sections, using many different optical potentials. These tests allowed us to establish that in general small variations of the real part mainly influence the shape of the cross section as a function of collision energy, while small variations of the imaginary part sensibly modify the absolute value of the cross section leaving substantially unchanged its energy dependence.

Taking into account these considerations, since methane−metastable neon is mainly charecterized by a weak vdW interaction, an increasing cross section as a function of collision energy must be expected, as effectively observed. In the case of methyl halides, due to the CT contribution, a strong anisotropy is present, corresponding to a weak vdW interaction for approaches at 90° and a more attractive interaction for approaches at 0° and 180°. Based on the electron exchange model of Penning ionization,[9] the most favorable situation for ionization is governed by the mutual overlap between the inner-shell hole of the metastable atom and the target orbital to be ionized. Comparing the electron distribution maps with the average van der Waals radius of CH_3Cl, as reported in Figure 7, one can easily argue that ionization takes place mainly when the metastable atom arrives within two preferential cones of approach, one on the CH_3 end and the other one on the opposite Cl end, where the interaction is strongly attractive (see Figure 8). This should lead to a decreasing trend of the total ionization cross section.

E. Branching Ratios. Regiospecific effects in ionization coupled with anisotropy of interaction can also qualitatively explain the observed energy dependence of branching ratios for the methyl halides. While no variation of branching ratios has been observed for $Ne^*(^3P_{2,0})-CH_4$ as a function of collision energy, for $Ne^*(^3P_{2,0})-CH_3X$ an increase of fragmentation is observed when collision energy increases. This point can be clarified making reference to Figure 8 and considering that the two effective approaches of the metastable atoms can lead to different populations of the electronic states of the CH_3X^+ ions primarily produced. Approaches toward the halogen atom cone can lead to a preferential formation of X and A states of CH_3X^+ ions, while those toward the CH_3 cone can lead to excited A and B states. Taking into account that the repulsive walls for approaches toward the part of chlorine atom are harder than those for approaches toward the methyl group, a deeper penetration at increasing collision energies for these last approaches is expected and therefore a more effective ionization into excited A and B states occurs. Since these states are dissociative with a full fragmentation to CH_3^+ and CH_2Cl^+ (or CH_2Br^+), a relative increase of fragment ions at increasing collision energies is expected as actually observed.

As mentioned above, Ohno and co-workers recently observed[11−13] different energy dependences of ionization cross sections for the population of different states of the ions primarily produced in $He^*(^3S)$ Penning ionization of molecules. This effect was correlated to the anisotropy of interaction and to the electron distribution of the molecule to be ionized. The same effect was also found by Siska and co-workers in a Penning ionization electron spectroscopy experiment on the $He^*(^1S)-N_2$ system.[14,15] Here, it is suggested that analogous effects occur in metastable neon−methyl halide collisions, where fragment ions are produced as a consequence of the population of excited states of the ion.

IV. Conclusions

In the present study, total and partial cross sections for Penning ionization of methyl chloride and methyl bromide by metastable neon atoms have been measured as a function of collision energy in the 0.040−0.15 eV range. The results have been discussed in comparison with those already obtained for methane. Total ionization and partial cross sections for the formation of CH_3X^+, CH_3^+, and CH_2X^+ (X = Cl, Br) show decreasing trends when the collision energy increases. In particular, branching ratios indicate that the production of fragment ions is favored at higher collision energies. This behavior is completely different than that of methane, where an increasing trend of total ionization cross sections was measured and no collisional energy dependence on branching ratios was observed.

A qualitative, but fully consistent, explanation has been given starting from the interaction potential between neon metastable atoms and methyl halide as estimated, for the prototype CH_3Cl molecule, on the basis of new correlation rules developed in our laboratory. Based on these rules which allow to estimate pure van der Waals but also charge-transfer contributions to intermolecular potentials, the $Ne^*(^3P_{2,0})-CH_3Cl$ anisotropy of interaction has been characterized by determining potential wells and equilibrium distances for five different angles of approach of the metastable atom to the target molecule.

It has been shown that the anisotropy of interaction is correlated with the behavior of total and partial ionization cross sections as a function of collision energy. In particular, the presence of an attractive interaction for *end-on* approaches to the target molecule is responsible of the decreasing trend of the total ionization cross sections. On the other hand, the presence of a softer repulsive wall around the methyl group is responsible of the increase of fragmentation of the CH_3Cl^+ molecular ions when collision energy increases. In fact, based on electron-exchange model of Penning ionization, the presence of a softer potential wall at the end of CH_3 allows a deeper penetration of the metastable atom, at increasing collision energies, toward the methyl group, leading to a more effective ionization into CH_3Cl^+ A and B excited states which fully dissociate to CH_3^+ and CH_2Cl^+.

Acknowledgment. This work has been partially supported by the EC through the SRMI European Network (HCMP), by the CNR Bilateral Agreement, and by a NATO Grant for International Collaboration. Jaime de Andres thanks the Spanish DGICYT for its help through program PB94-0909.

References and Notes

(1) Brunetti, B.; Vecchiocattivi, F. In *Ion Clusters*, Ng, C., Baer, T., Powis, I., Eds.; Wiley & Sons Ltd.: New York, 1993; pp 359−445 and references therein.
(2) Siska, P. E. *Rev. Mod. Phys.* **1993**, *65*, 337 and references therein.
(3) Nakamura, H. *J. Chem. Phys. Jpn.* **1969**, *26*, 1973; **1971**, *31*, 574.
(4) Miller, W. H. *J. Chem. Phys*. **1970**, *52*, 3563.
(5) Vojtik, J. *Chem. Phys.* **1996**, *209*, 367 and references therein.
(6) Bevsek, H. M.; Siska, P. E. *J. Chem. Phys.* **1995**, *102*, 1934.
(7) Ishida, T.; Horime, K. *J. Chem. Phys.* **1996**, *105*, 5380.
(8) Ishida, T. *J. Chem. Phys.* **1995,** *102*, 4169; **1996**, *105*, 1392.
(9) Hotop, H.; Niehaus, A. *Z. Phys.* **1969**, *228*, 68.
(10) Ohno, K.; Mutoh, H.; Harada, Y. *J. Am. Chem. Soc.* **1983**, *105*, 4555. Mitsuke, K.; Takami, T.; Ohno, K. *J. Chem. Phys.* **1989**, *91*, 1618. Ohno, K.; Harada, Y. In *Theoretical Models of Chemical Bonding*; Maksic, Z. B., Ed.; Springer-Verlag: Berlin, 1991; Part 3, pp 199−233.

(11) Ohno, K.; Takami, T.; Mitsuke, K.; Ishida, T. *J. Chem. Phys.* **1991**, *94*, 2675. Takami, T.; Mitsuke, K.; Ohno, K. *J. Chem. Phys.* **1991**, *95*, 918.

(12) Pasinszki, T.; Yamakado, H.; Ohno, K. *J. Phys. Chem.* **1995**, *99*, 14678.

(13) Yamakado, H.; Yamauchi, M.; Hoshino, S.; Ohno, K. *J. Phys. Chem.* **1995**, *99*, 17093.

(14) Dunlavy, D. C.; Martin, D. W.; Siska, P. E. *J. Chem. Phys.* **1990**, *93*, 5347.

(15) Dunlavy, D. C.; Siska, P. E. *J. Phys. Chem.* **1996**, *100*, 21.

(16) Aguilar, A.; Brunetti, B.; Falcinelli, S.; Gonzalez, M.; Vecchiocattivi, F. *J. Chem. Phys.* **1992**, *96*, 433. Brunetti, B.; Cambi, R.; Falcinelli, S.; Farrar, J. M.; Vecchiocattivi, F. *J. Phys. Chem.* **1993**, *97*, 11877. Brunetti, B.; Falcinelli, S.; Paul, S.; Vecchiocattivi, F.; Volpi, G. G. *J. Chem. Soc., Faraday Trans.* **1993**, *89*, 1505. Appolloni, L.; Brunetti, B.; Vecchiocattivi, F.; Volpi, G. G. *J. Phys. Chem.* **1988**, *92*, 918. Brunetti, B.; Falcinelli, S.; Sassara, A.; de Andres, J.; Vecchiocattivi, F. *Chem. Phys.* **1996**, *209*, 205.

(17) Aguilar, A.; Brunetti, B.; Gonzalez, M.; Vecchiocattivi, F. *Chem. Phys.* **1990**, *145*, 211.

(18) Eland, J. H. D.; Frey, R.; Kuestler, A.; Schulte, H.; Brehm, B. *Int. J. Mass Spectrom. Ion Phys.* **1976**, *22*, 155.

(19) Gallagher, J. W.; Brion, C. E.; Samson, J. A. R.; Langhoff, P. W. *J. Phys. Chem. Ref. Data* **1988**, *17*, 9 and references therein.

(20) Backx, C.; Van der Wiel, M. J. *J. Phys. B* **1975**, *18*, 3020.

(21) Sieck, L. W.; Gorden, R., Jr. *Chem. Phys. Lett.* **1973**, *19*, 509.

(22) Au, J. W.; Cooper, G.; Brion, C. E. *Chem. Phys.* **1993**, *173*, 241.

(23) Cermak, V.; Herman, Z. *Collect. Czech. Chem. Commun.* **1965**, *30*, 169.

(24) Muschlitz, E. E.; Weiss, M. J. In *Mass Spectrometry of Organic Ions*; McLafferty, F. W., Ed.; Academic Press: New York, 1963.

(25) Tosi, P.; Bassi, D.; Brunetti, B.; Vecchiocattivi, F. *Int. J. Mass Spectrom. Ion Processes* **1995**, *149/150*, 345.

(26) Turner, D. W.; Baker, C.; Baker, A. D.; Brundle, C. R. *Molecular Photoelectron Spectroscopy*; Wiley-Interscience: New York, 1970 and references therein.

(27) Frey, R. F.; Davidson, E. R. *J. Chem. Phys.* **1988**, *88*, 1775.

(28) Stockbauer, R. *J. Chem. Phys.* **1973**, *58*, 3800.

(29) Bombach, R.; Dannacher, J.; Stadelman, J. P. *Int. J. Mass Spectrom. Ion Processes* **1984**, *58*, 217.

(30) Dunning, T. H., Jr. *J. Chem. Phys.* **1971**, *55*, 716.

(31) McLean, A. D.; Chandler, G. S. *J. Chem. Phys.* **1980**, *72*, 5630.

(32) Ahlrichs, R.; Taylor, P. R. *J. Chem. Phys.* **1981**, *78*, 315.

(33) Guest, M. F.; Sherwood, P. *GAMESS-UK, User Guide and Reference Manual*; SERC Daresbury Laboratory, UK, 1992.

(34) Lane, I. C.; Powis, I. *J. Phys. Chem.* **1993**, *97*, 5803.

(35) Brion, C. E.; Stewart, W. B.; Yee, D. S. C.; Crowley, P. *J. Electron Spectrosc. Relat. Phenom.* **1981**, *23*, 45.

(36) Cambi, R.; Cappelletti, D.; Liuti, G.; Pirani, F. *J. Chem. Phys.* **1991**, *95*, 1852.

(37) Liuti, G.; Pirani, F. *Chem. Phys. Lett.* **1985**, *122*, 2154.

(38) Cappelletti, D.; Liuti, G.; Pirani, F. *Chem. Phys. Lett.* **1991**, *183*, 297.

(39) Aquilanti, V.; Cappelletti, D.; Pirani, F. *Chem. Phys*. **1996**, *209*, 299.

(40) Pirani, F. *Discuss. Faraday Soc*. **1994**, *97*, 327.

(41) Pirani, F.; Cappelletti, D.; Aquilanti, V. In *Molecular Physics and Hypersonic Flows*; Capitelli, M., Ed.; Kluwer: Dordrecht, 1996.

(42) Aquilanti, V.; Cappelletti, D.; Pirani, F. *J. Chem. Phys*. **1997**, *106*, 5043; *Chem. Phys. Lett.* **1997**, *271*, 216.

(43) Hirschfelder, J. O.; Curtiss, C. F.; Bird, R. B. *The Molecular Theory of Gases and Liquids*, Wiley: New York, 1954.

(44) Standard, J. M.; Certain, P. R. *J. Chem. Phys*. **1985**, *83*, 3002. Koutselos, A. D.; Mason, E. A. *J. Chem. Phys.* **1986**, *85*, 2154.

(45) Dick, B. G.; Overhauser, A. W. *Phys. Rev.* **1958**, *112*, 90. Hafemeister, D. W.; Flygare, W. H. *J. Chem. Phys.* **1965**, *43*, 795. Hafemeister, D. W.; Zahet, J. D. *J. Chem. Phys.* **1967**, *47*, 1428.

(46) Krauss, K. *J. Chem. Phys.* **1977**, *67*, 1712.

(47) Denbigh, K. G. *Trans. Faraday Soc*. **1940**, *36*, 936.

(48) Magee, J. L. *J. Chem. Phys*. **1940**, *8*, 687.

(49) Grice, R.; Herschbach, D. R. *Mol. Phys*. **1974**, *27*, 158.

(50) Tokue, I.; Sakai, Y.; Yamasaki, K. *J. Chem. Phys.* **1997**, *106*, 4491.

(51) Gregor, R. W.; Siska, P. E. *J. Chem. Phys.* **1981**, 74, 1078.

(52) Niehaus, A. *Adv. Chem. Phys.* **1981**, *45*, 399 and references therein.

(53) van den Berg, F. T. M.; Schoenenberg, J. H. M.; Beijerinck, H. C. W. *Chem. Phys*. **1987**, *115*, 359.